Methylation of Histone H3 by Coactivator-Associated Arginine Methyltransferase 1†

Brandon T. Schurter,‡ Stephen S. Koh,§ Dagang Chen,§ Gerard J. Bunick,|| Joel M. Harp,|| B. Leif Hanson,|| Agnes Henschen-Edman,‡ Douglas R. Mackay,‡ Michael R. Stallcup,§ and Dana W. Aswad*,‡

Department of Molecular Biology and Biochemistry, University of California, Irvine, California 92697, Department of Pathology, University of Southern California, Los Angeles, California 90089, and Oak Ridge National Laboratory, Oak Ridge, Tennessee 37831

Received November 15, 2000; Revised Manuscript Received March 5, 2001

ABSTRACT: The preferential in vitro methylation of histone H3 by coactivator-associated arginine methyltransferase 1 (CARM1) has been proposed as a basis for its ability to enhance gene transcription [Chen, D., et al. (1999) *Science 284*, 2174−2177]. To further evaluate the significance of H3 methylation, we studied the kinetics and site specificity of its modification by CARM1. Affinity-purified CARM1 methylated recombinant chick H3, which is free of posttranslational modifications, and calf thymus H3, which is heterogeneous with regard to preexisting modifications, equally well, exhibiting a V_{max} of 4500 pmol min^{-1} (mg of enzyme)$^{-1}$ and an apparent K_m for H3 of ≤ 0.2 μM. The catalytic efficiency (k_{cat}/K_m) of CARM1 toward H3 was at least 1000 times that toward R1 (GGFGGRGGFGG-amide), a highly effective substrate for protein arginine methyltransferase 1. Peptide mapping of ^{3}H-methyl-labeled H3 indicated methylation at Arg-2, Arg-17, and Arg-26 in the N-terminal region and at one or more of four arginines (128/129/131/134) at the C-terminus. Two of the N-terminal sites, Arg-17 and Arg-26, occur in the sequence KAXRK and appear to be more efficiently methylated than Arg-2. CARM1 catalyzed formation of N^G,N^G-dimethylarginine (asymmetric) but little or no N^G,N'^G-dimethylarginine (symmetric) and no form of methyllysine. Amino acid analysis of untreated calf thymus H3 revealed that 3.7% of the molecules naturally contain asymmetric dimethylarginine and/or monomethylarginine. Our findings support the hypothesis that methylation of H3 may be involved in the mechanism of transcriptional coactivation by CARM1 of genes whose expression is under the control of nuclear receptors.

Coactivator-associated arginine methyltransferase 1 (CARM1)[1] is a recently discovered component of the transcriptional coactivator machinery that mediates gene activation in response to steroids and related hormones that interact directly with DNA-binding nuclear hormone receptors (*1*). CARM1 was originally discovered in a yeast two-hybrid screen for proteins that interact strongly with the glucocorticoid receptor interacting protein 1 (GRIP1; also known as TIF2), a member of the p160 family of coactivators that includes SRC-1 and pCIP/RAC3/ACTR/AIB1/TRAM1. In transient transfection assays, p160 coactivators enhance the ability of hormone-activated nuclear receptors to activate expression of a reporter gene controlled by appropriate nuclear receptor response elements (*2*). In the presence of a p160 coactivator, CARM1 caused a further enhancement of nuclear receptor activity (*1*). The cDNA sequence of CARM1 encodes a 66 kDa protein with significant sequence homology to the widely distributed protein arginine methyltransferase 1 (PRMT1/HRMT1) and its yeast homologue RMT1/HMT1/ODP1, well-studied protein arginine methyltransferases responsible for the formation of dimethylarginine in proteins such as nucleolin, fibrillarin, and heterogeneous nuclear ribonucleoproteins that are involved in the processing and transport of RNA (*3*−*6*).

The p160 transcriptional coactivators mediate their effects in part via interaction with additional coactivators such as CREB binding protein, which possess histone acetyltransferase activity. Histone acetylation appears to play a critical role in remodeling chromatin structure in a way that facilitates transcription (*7*−*9*). Since histones are also methylated in vivo on the side chains of lysine and arginine residues (*10, 11*), and since CARM1 is homologous to known protein *N*-methyltransferases, the ability of affinity-purified CARM1 to methylate the core histones H2a, H2b, H3, and H4 in vitro was investigated (*1*). When CARM1 was incubated with the individual calf thymus histones, significant methylation of histones H2a and H3 was observed, with little or no methylation of histones H2b or H4. When CARM1 was presented with a mixture of unfractionated calf thymus core histones, it preferentially methylated histone H3.

† This work was supported by USPHS Grants NS17269 (D.W.A.), DK55274 (M.R.S.), and GM 29181 (G.J.B.), by NASA Grant NAG8-1568 (G.J.B.), by the Office of Biological and Environmental Research, DOE contract DE-AC05-00OR22725 with UT Battele, LLC (G.J.B.), and by USPHS Predoctoral Training Grant AG00093 (S.S.K.).

* To whom correspondence should be addressed. Telephone: (949) 824-6866. Fax: (949) 824-8551. E-mail: dwaswad@uci.edu.

‡ Department of Molecular Biology and Biochemistry, University of California.

§ Department of Pathology, University of Southern California.

|| Oak Ridge National Laboratory.

[1] Abbreviations: CARM1, coactivator-associated arginine methyltransferase 1; PRMT1, protein arginine methyltransferase 1; GST, glutathione *S*-transferase; MMA, N^G-monomethyl-L-arginine; ADMA, N^G,N^G-dimethylarginine (asymmetric); SDMA, N^G,N'^G-dimethyl-L-arginine (symmetric); AdoMet, *S*-adenosyl-L-methionine; HPLC, high-performance liquid chromatography; TFA, trifluoroacetic acid; TCA, trichloroacetic acid; MALDI-TOF, matrix-assisted laser desorption ionization−time of flight.

10.1021/bi002631b CCC: $20.00
Published on Web 04/05/2001

Table 1: Methylation Reaction Conditions[a]

method	volume (μL)	CARM1 (μg)	^{3}H-AdoMet μM	^{3}H-AdoMet dpm/pmol	temp (°C)	time (min)	stop solution μL	stop solution composition
A	50	0.12	7.4	32 000	30	30	25	1.5% (v/v) TFA, 15% (v/v) acetonitrile
B	100	2.4	7.4	32 000	30	60	25	3.0% (v/v) TFA, 15% (v/v) acetonitrile
C	50	0.08	10	4 300	37	5	800	10% (w/v) TCA
D	150	16	200	1 300	37	90	400	10% (w/v) TCA
E	150	8	200	1 300	37	15	400	10% (w/v) TCA

[a] All reactions were carried out in 20 mM Tris-HCl (pH 8.0), 0.2 M NaCl, and 0.4 mM EDTA.

To further evaluate the physiological significance of histone H3 methylation, we investigated the kinetic properties that characterize this reaction and the locations of the preferred methylation sites. Quantitative information on the kinetic properties, stoichiometries, and site specificities that characterize posttranslational modification reactions often can help to distinguish physiologically important substrates from those which are not. The location of CARM1-directed methylation sites in histone H3 is of special interest since this histone is already known to be modified via lysine acetylation, lysine N-methylation, and serine phosphorylation at several distinct sites within the flexible N-terminal region (reviewed in refs *7* and *8*). These neighboring modifications may work in conjunction with each other to form a complex code that integrates input from several activation pathways leading to the appropriate RNA output. The studies reported here show that CARM1 methylates H3 with a high degree of efficiency at specific sites located near the N- and C-termini.

EXPERIMENTAL PROCEDURES

Materials. The synthetic peptides R1 (GGFGGRGGFG-amide) and K1 (GGFGGKGGFG-amide) were described previously (*12*). Glutathione *S*-transferase:coactivator-associated arginine methyltransferase fusion protein (GST-CARM1) was prepared as described previously (*1*). Calf thymus histone H3 and endoproteinases Glu-C and Lys-C were purchased from Boehringer-Mannheim. N^G-Monomethyl-L-arginine (MMA) was from Calbiochem. N^G,N^G-dimethyl-L-arginine (asymmetric dimethylarginine; ADMA) was from Chemical Dynamics Corp., Plainfield, NJ. N^G,N'^G-dimethyl-L-arginine (symmetric dimethylarginine; SDMA), N^ϵ-dimethyl-L-lysine, and N^ϵ-trimethyl-L-lysine were obtained from Sigma Chemical Co. *S*-Adenosyl-L-[*methyl*-^{3}H]methionine ([*methyl*-^{3}H]AdoMet; 14−15 Ci/mmol) was purchased from Dupont NEN and, when necessary, adjusted to lower specific activity by dilution with unlabeled AdoMet (Sigma Chemical Co.) that had been purified on carboxymethylcellulose prior to use (*13*).

The chicken H3 gene, cloned into a pET13-derived vector, was expressed as an insoluble product in *Escherichia coli* strain BL21(DE3). Protein expression was induced with 0.4 mM IPTG followed by 4−5 h incubation at 37 °C. Cells were harvested by centrifugation and lysed with three cycles of freezing and thawing in liquid nitrogen. Inclusion bodies were prepared and solubilized in 7 M guanidine hydrochloride and 20 mM sodium acetate, pH 5.2. Histone H3 was purified by gel filtration on a Sephacryl S-200 (Pharmacia) column equilibrated in 8 M urea and 20 mM sodium acetate, pH 5.2, followed by cation-exchange chromatography on Mono-S (Pharmacia) using a linear NaCl gradient in 8 M urea and 20 mM sodium acetate, pH 5.2. Purified H3 was dialyzed extensively versus 0.1 mM phenylmethanesulfonyl fluoride and lyophilized. The protein was homogeneous as judged by SDS−PAGE. H3 solubilized and purified in this manner has been shown to form structurally normal nucleosomes when combined in the correct ratio with other recombinant core histones (*14*).

Methylation Reactions. Methylation reactions (45−150 μL) contained 20 mM Tris-HCl (pH 8.0), 0.2 M NaCl, 0.4 mM EDTA, affinity-purified GST-CARM1, methyl acceptor, and [*methyl*-^{3}H]AdoMet. Additional details of individual reactions are presented in Table 1, which is referenced in the appropriate sections of the text and figure legends.

High-Performance Liquid Chromatography (HPLC). HPLC was carried out with a Gilson dual-pump gradient system employing a 1.5 mL high-pressure mixer. Postcolumn UV absorbance was monitored on-line with a Gilson 117 detector. Postcolumn fluorescence was monitored on-line with a Gilson 122 fluorometer using excitation and emission wavelengths of 340 and 455 nm, respectively. Details of individual HPLC separation conditions are presented in Table 2, which is referenced in the appropriate sections of the text and figure legends.

Analysis of ^{3}H-Labeled Amino Acids. Calf thymus H3 (42 μg) was ^{3}H-methylated according to Table 1, method B, and then purified by HPLC according to Table 2, method B. Peak fractions were pooled, dried in a vacuum centrifuge, and subjected to acid hydrolysis in 0.5 mL of 6 N HCl by heating at 112 °C for 20 h. The hydrolysate was dried under vacuum and resuspended in 100 μL of water. For HPLC analysis of [^{3}H]methyl amino acids, a 20 μL sample of the hydrolysate was derivatized with 5 μL of *o*-phthaldialdehyde reagent (*15*) and then analyzed by HPLC according to method C in Table 2. For analysis of [^{3}H]methyl amino acids by thin-layer chromatography, approximately 8 μL of hydrolysate was mixed with 1 nmol each of MMA, ADMA, and SDMA standards and applied as a small spot to a cellulose thin-layer sheet (EM Separations; catalog no. 5577). Amino acids were separated by ascending chromatography in pyridine:acetone:ammonium hydroxide:water, 15:9:1.5:6, and visualized with ninhydrin (*10*). The lane containing the hydrolysate was cut into sections of approximately 0.5 cm. The cellulose coatings were scraped into individual vials for determination of ^{3}H by liquid scintillation counting.

Proteolytic Digestion. Endoproteinase Glu-C digestions were carried out at a substrate:Glu-C ratio of approximately 15:1 by weight at 37 °C for 4 h in 50 mM ammonium acetate (pH 4.0) and then stopped by addition of trifluoroacetic acid (TFA) to a final concentration of 0.3%. Endoproteinase Lys-C digestions were carried out at a substrate:Lys-C ratio

Table 2: HPLC Conditions[a]

method	column	solvent A	solvent B	gradient program and flow rate
A	Aquapore RP-300, 2.1 × 30 mm, Brownlee no. CO3-032	0.1% TFA	0.09% TFA in 50% acetonitrile	10% B, 1 min; 10−40% B, 7 min; 40% B, 2 min (1.0 mL/min)
B	Aquapore RP-300, 4.6 × 30 mm, Brownlee no. CO3-GU	0.3% TFA	0.3% TFA in 100% acetonitrile	20% B, 1 min; 20−80% B, 5 min; 80% B, 10 min (1.0 mL/min)
C	Dynamax Microsorb AAAnalysis, Type O kit, Rainin no. R0080OPAK3	79% 50 mM sodium acetate, pH 5.9; 20% methanol; 1% tetrahydrofuran	20% 50 mM sodium acetate, pH 5.9; 80% methanol	5% B, 2 min; 5−40% B, 20 min; 40% B, 2 min (1.0 mL/min)
D	Aquapore RP-300,[b] 4.6 × 100 mm, Brownlee no. CO3-102	0.3% TFA	0.3% TFA in 100% acetonitrile	5% B, 2 min; 5−50% B, 100 min (1.0 mL/min)
E	Velosep RP-18, 3.2 × 100 mm, Brownlee no. V18-103	0.1% TFA	0.09% TFA in 50% acetonitrile	0% B, 2 min; 0−60% B, 60 min; 60−100% B, 5 min; 100% B, 2 min (0.5 mL/min)

[a] Solvent compositions are expressed as solute percent (v/v) in water unless stated otherwise. [b] This column was fitted with a 4.6 × 30 mm Aquapore BU-300 guard cartridge (Brownlee no. BO3-GU).

of approximately 20:1 at 37 °C for 24 h in 40−160 mM Tris-HCl (pH 8.6) and then stopped with TFA as above.

Initial Rate Kinetics. Methylation reactions were carried out as described in Table 1, method C, using various concentrations of calf thymus or recombinant histone H3. After addition of 100 μg of γ-globulin as carrier, stopped reactions were incubated on ice for 15 min followed by a brief centrifugation to pellet the protein. The supernatants were aspirated, and the pellets were dissolved in 50 μL of 88% formic acid. After the TCA precipitation step was repeated, the formic acid solubilized pellets were subjected to liquid scintillation counting for evaluation of ^{3}H incorporation.

Liquid Scintillation Counting. Measurements of ^{3}H were made in Liquiscint (National Diagnostics, Inc.) using a Beckman LS-6500 counter. Counting efficiency was determined by the channel ratio method based on a series of chloroform-quenched standards of [^{3}H]toluene.

Mass Spectrometry. Mass spectra were recorded on a Voyager DE-Pro matrix-assisted laser desorption ionization−time of flight (MALDI-TOF) mass spectrometer equipped with a nitrogen laser operating at 337 nm (PerSeptive Biosystems). Typically, 0.5 μL of the analyte was mixed with 0.5 μL of saturated α-cyano-4-hydroxycinnamic acid in 60% acetonitrile/0.3% TFA and spotted onto the sample plate. All spectra were acquired in the positive ion mode. Data were integrated with GRAMS/386 software (Galactic Industries Corp., Salem, NH).

Radiosequencing of Methylated H3. Methylation of recombinant H3 was carried out according to Table 1, method D, except that the reaction was stopped by addition of 25 μL of 2.1% TFA. The ^{3}H-methylated histone was separated from the other components of the reaction by HPLC, method B in Table 2, except that the 2.1 mm diameter RP-300 column described in method A was used. The histone peak fractions were pooled and reduced in volume to ca. 50 μL in a vacuum centrifuge. A portion of the sample containing 405 pmol of [^{3}H]methyl was then subjected to 20 cycles of automated Edman degradation in a Hewlett-Packard G1005A sequenator. The PTH-amino acids from each cycle were collected for measurement of ^{3}H by liquid scintillation counting.

Protein Determination. The concentrations of GST-CARM1 stock solutions were estimated by subjecting samples to SDS−PAGE and comparing the Coomassie blue stained bands with standards of bovine serum albumin run on the same gel. The concentrations of histone stock solutions were determined by the method of Lowry (*16*). Concentrations of the R1 and K1 peptides were based on the dry weight of the purified peptides.

RESULTS

Methylation of R1 and K1 Synthetic Peptides. The first indication that CARM1 might be a protein arginine methyltransferase emerged from the discovery that the CARM1 cDNA shows a high degree of homology to PRMT1 (*1*), an enzyme with high specificity for -GGRGG- and related Arg/Gly-rich sequences found in many RNA-binding proteins. To determine if CARM1 and PRMT1 recognize similar sequences, and to test the relative specificity of CARM1 for arginine vs lysine methylation, we assayed the ability of GST-CARM1 to methylate peptides R1 (GGFGGRGGFG-amide) and K1 (GGFGGKGGFG-amide), which were available in our laboratory from a previous study on the specificity of protein *N*-methyltransferase(s) in rat PC12 cells (*12*). The peptides were incubated with GST-CARM1 in the presence of [^{3}H]Adomet and then separated from the unreacted [^{3}H]-Adomet by reversed-phase HPLC. R1 was methylated but K1 exhibited little or no methylation (Figure 1). The peak of radiolabeled R1 eluted later than the UV peak of unmethylated R1 because methylation increased the hydrophobicity of the peptide. We calculated that only 0.003% of the R1 peptide (0.054 pmol out of 2000 pmol total injected) was methylated, which explains why a UV peak corresponding to the methylated subfraction of R1 is not visible in the trace shown in panel A. Because the level of methyl incorporation was so low, we considered the possibility that the radiolabeling may have resulted from tritium exchange with the arginine side chain rather than enzymatic modification. To address this, we also ran a blank in which only CARM1 was omitted from the reaction. This blank reaction (not shown) gave results indistinguishable from the blank shown in panel C, in which R1 only was omitted from the methylation reaction.

The specific activity of CARM1 increased with R1 concentration (Table 3), but the activity was low: 55 pmol min^{-1} (mg of enzyme)$^{-1}$ at 150 μM R1. In contrast, we found that GST-PRMT1 methylated R1 with a specific activity of

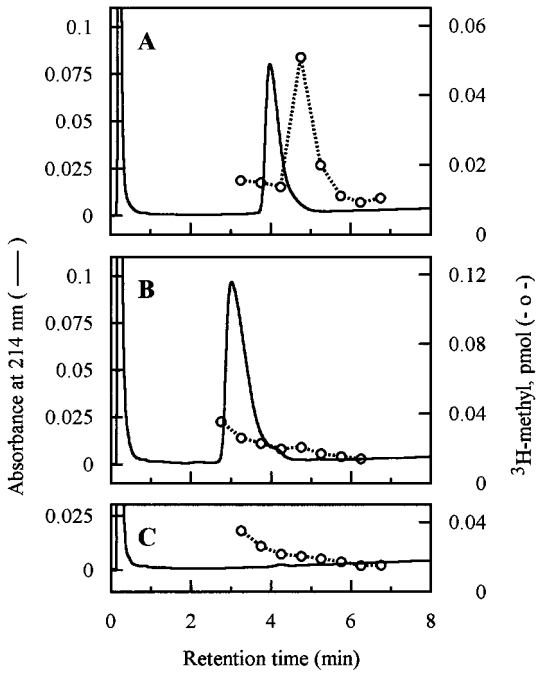

FIGURE 1: Methylation of R1 (GGFGGRGGFG-amide) and K1 (GGRGGKGGFG-amide) by GST-CARM1. Equal concentrations (150 μM) of the two peptides were ^{3}H-methylated in separate reactions according to method A in Table 1 and then separated from unreacted [*methyl*-^{3}H]AdoMet by HPLC using method A in Table 2. For the R1 peptide (panel A), 27% of the methylation reaction was taken for HPLC. For the K1 peptide (panel B) and the blank (panel C; reaction containing no peptide), 53% of each reaction was taken. The *Y*-axis on the right side of panel A is scaled differently than that for panels B and C to compensate for the smaller sample size.

Table 3: Specific Activity of CARM1 toward R1, K1, and Histone H3[a]

methyl acceptor	concn (μM)	CARM1 activity (pmol min^{-1} mg^{-1})
R1 (GGFGGRGGFG-amide)	22	13
	150	55
K1 (GGFGGKGGFG-amide)	22	<1
	150	<1
H3, chick recombinant	1.0	4500
H3, calf thymus	1.0	4500

[a] Methylation of the R1 and K1 peptides was carried out as described in the legend to Figure 1. The histone H3 data are taken from Figure 6.

3100 pmol min^{-1} mg^{-1} under the same assay conditions. These results suggested that CARM1 is selective for arginine, but that its substrate specificity is quite different from that of PRMT1.

Nature of the Methylated Amino Acids Recovered from Histone H3 after Methylation by CARM1. After our study of R1 and K1 methylation, we found that CARM1 exhibits a robust activity and preference for methylation of histone H3 in a commercial preparation of calf thymus core histones (*1*). To further investigate the amino acid specificity of CARM1, we carried out an amino acid analysis of ^{3}H-methylated calf thymus histone H3 as described in Experimental Procedures. Reversed-phase HPLC analysis of the hydrolysate (Figure 2) indicated that virtually all of [^{3}H]-methyl label coeluted with MMA and/or ADMA. No significant label was found in the position of mono-, di-, or trimethyllysine. To determine the distribution of label among

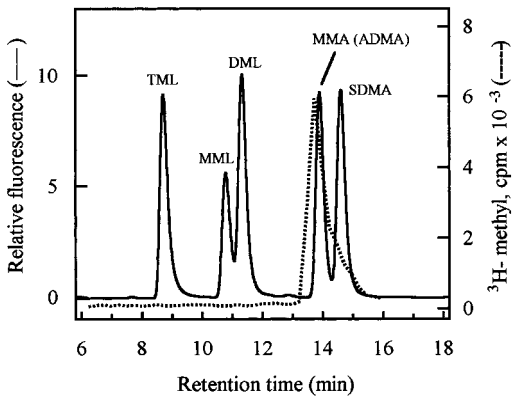

FIGURE 2: HPLC of amino acids derived from ^{3}H-methylated histone H3. An acid hydrolysate representing 430 pmol of calf thymus H3 methylated by GST-CARM1 was reacted with *o*-phthaldialdehyde, and the derivatized amino acids were separated by reversed-phase HPLC as described in Experimental Procedures. The dashed line shows the distribution of radiolabel from the acid hydrolysate, and the solid line shows the separation of five amino acid standards chromatographed in a separate run. ADMA, which coelutes with MMA, was not present in the standard run shown here.

the three common forms of methylarginine, a sample of the same hydrolysate was analyzed by thin-layer chromatography (Figure 3), which revealed ^{3}H-labeling of both ADMA and MMA in a ratio of 2.4 to 1. In agreement with the HPLC results, little or no [^{3}H]methyl was associated with SDMA. These results confirmed that CARM1 is an arginine-specific methyltransferase and that the major products are MMA and ADMA, similar to what is found when PRMT1/HRMT1L2 and its yeast homologue RMT1/HMT1/ODP1 methylates its Gly/Arg-rich substrates (*17*, *18*).

Preexisting Modifications in Calf Thymus H3. In an initial attempt to determine the specific sites of H3 methylation catalyzed by CARM1, calf thymus H3 was ^{3}H-methylated with CARM1 and digested with endoproteinase Glu-C. Peptides were then separated by reversed-phase HPLC (method D in Table 2), and fractions were collected to measure [^{3}H]methyl incorporation relative to the UV absorption profile. Results (not shown) indicated that 60−70% of the [^{3}H]methyl was associated with Glu-C fragment 1−50, which includes the amino-terminal domain of H3 that is known to be the site of numerous posttranslational modifications. To more precisely locate the methylation sites, this Glu-C fragment was subdigested with endoproteinase Lys-C in expectation that it would produce eight distinct peptides, five of which would contain at least one arginine. Unfortunately, both the peptide elution profile and the distribution of radiolabel were much more complex than anticipated, suggesting that that either the Lys-C was not acting as predicted or that the amino-terminal domain of calf thymus H3 was heterogeneous, perhaps due to preexisting posttranslational modifications.

MALDI-TOF mass spectrometry of the 1−50 fragment of calf thymus H3 (unmethylated by CARM1) revealed a high degree of heterogeneity, much of which was apparently due to methylation and/or acetylation as indicated by the regular spacing of major peaks every 14 ± 0.2 mass units (Figure 4A). Methylation adds a mass of 14 to a peptide, while acetylation adds a mass of 42, the numerical equivalent of exactly three methyl groups. Early studies on the amino

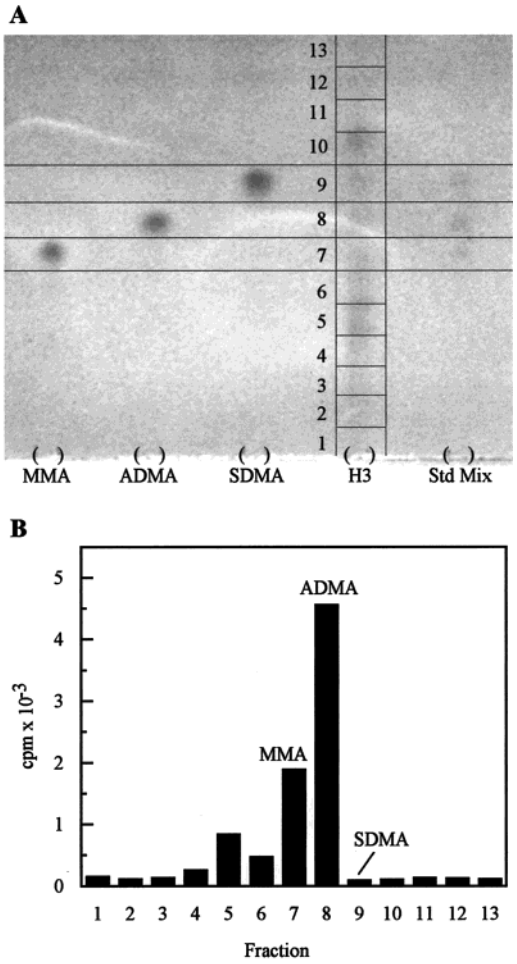

FIGURE 3: Thin-layer chromatography of amino acids derived from ^{3}H-methylated histone H3. (A) A portion (representing 260 nmol of H3) of the acid hydrolysate used in Figure 2 was subjected to thin-layer chromatography, lane 4 (H3), along with methylarginine standards, lanes 1−3 and 5. The ninhydrin-stained chromatogram is shown. Details of the chromatography are described in Experimental Procedures. Sections of lane 4 cut for liquid scintillation counting are numbered to correspond with panel B. (B) Distribution of radiolabel along lane 4.

acid sequence of calf thymus H3 revealed that calf thymus H3 contains significant levels of mono-, di-, and trimethyllysine at positions 9 and 27 and acetyllysine at positions 14 and 23 (*19*). A random distribution of methyl and acetyl groups at just these sites predicts up to 64 possible mass variants. From the pattern seen in Figure 4A, there is evidence for at least 10 variants, with 6 of these (the mass-labeled peaks) being most prominent. One of the most common variants seen in Figure 4A has a mass (5445.5) that is 103.3 mass units larger than that expected for the unmodified peptide (5342.2). This mass difference is sufficient to accommodate up to two acetyl groups, up to seven methyl groups, or various combinations of these two modifications. Because the mass difference is not an exact multiple of 14, it would appear that the calf thymus histone contains at least one modification other than methylation or acetylation. This heterogeneity explains the unexpected complexity we observed in the Lys-C peptide map: methyl and acetyl groups alter the retention time of short peptides due to changes in hydrophobicity and are also expected to greatly alter the expected cleavage pattern produced by Lys-C digestion.

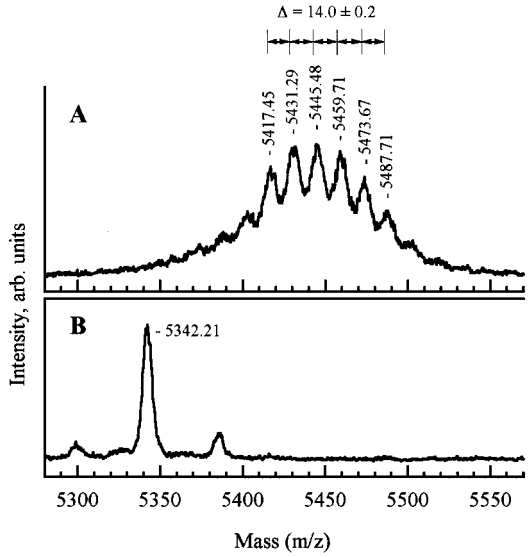

FIGURE 4: Mass spectra of the 1−50 peptides obtained by Glu-C digestion of histone H3. Calf thymus H3 (A) and recombinant chicken H3 (B) were digested with endoproteinase Glu-C as described in Experimental Procedures. The 1−50 peptide from each digest was isolated by HPLC as described in Table 2, method D. Mass spectra were obtained in the linear mode, and average masses are shown. Approximately 55 and 15 pmol of peptide were analyzed in panels A and B, respectively. Multiple peaks, differing by 14 mass units, indicate that calf thymus H3, as isolated, is highly heterogeneous with regard to methylation within the 1−50 region. The expected mass $[M + H]^+$ for unmodified H3(1−50) is 5342.2 in both species.

To circumvent the heterogeneity problem, we turned to recombinant H3 on the assumption that little or no post-translational modification occurs during its expression in *E. coli*. Indeed, the recombinant chick H3 1−50 peptide had exactly the expected mass for the unmodified peptide (Figure 4B).

Calf Thymus H3 Contains ADMA and/or MMA. If histone H3 is a substrate for CARM1 in vivo, one might expect to find at least small amounts of methylarginine in acid hydrolysates of the naturally occurring histone. To investigate this point, we subjected calf thymus H3 to acid hydrolysis followed by amino acid analysis using the *o*-phthaldialdehyde/HPLC method. On first inspection, the HPLC results from 125 pmol of H3 indicated no obvious peak in the region where the ADMA/MMA standard runs (results not shown); however, expansion of this region to reveal minor peaks did reveal two possible candidates, one eluting at 17.2−17.4 min and one at 17.6−17.8 min (Figure 5B). When the same hydrolysate was mixed with 3.3 pmol of ADMA standard prior to analysis, the 17.2−17.4 min peak was selectively amplified (Figure 5C). In contrast, a hydrolysate of recombinant chick H3 showed no minor peaks in this region (Figure 5A).

By measuring the change in peak area resulting from inclusion of the ADMA standard, we calculated that approximately 3.7% of calf thymus H3 molecules contain ADMA and/or MMA. A similar analysis of other calf thymus core histones (all from Boehringer-Mannheim) revealed that H2a, H2b, and H4 contain 0.9%, <0.1%, and 0.7% ADMA/MMA, respectively. These results suggest that methylation of H3 by CARM1 and/or other arginine methyltransferase occurs in vivo on a subpopulation of mammalian H3 molecules.

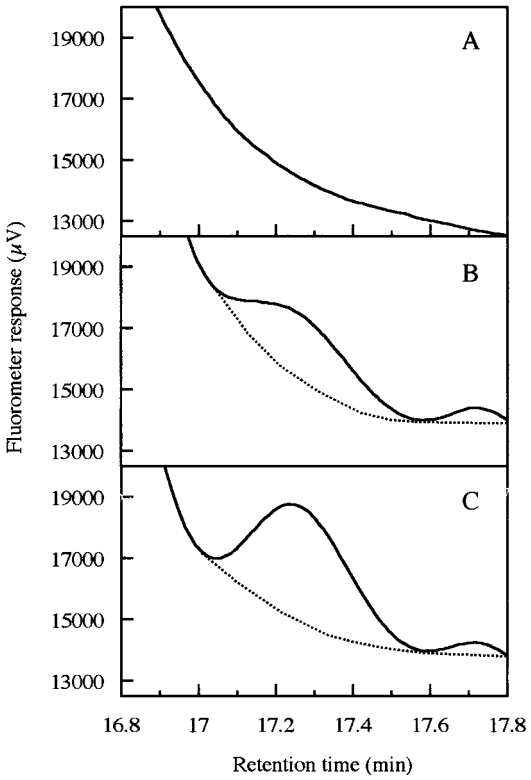

FIGURE 5: Identification of ADMA and/or MMA in acid hydrolysates of calf thymus H3. Acid hydrolysis and amino acid analysis of untreated histone H3 samples were a carried out as described under Analysis of ^{3}H-Labeled Amino Acids in Experimental Procedures. For the series of chromatograms shown here, a standard of ADMA run alone was found to elute at 17.2 ± 0.2 min. Panel A shows the ADMA region resulting from analysis of 125 pmol of recombinant chick H3, which serves as a control that is presumed to be free of methylarginine. Panel B shows the result obtained from 125 pmol of untreated calf thymus H3. Panel C is the same as panel B except that 3.3 pmol of ADMA standard was mixed with the H3 sample prior to analysis.

Methylation Kinetics of Histone H3. Initial rate studies on the methylation of histone H3 by CARM1 were carried out to estimate K_m and V_{max} values. This information was of interest in that it bears upon the possible physiological relevance of H3 methylation and provides important insights that help to optimize conditions for extensive methylation of H3 needed for site analysis. We were also interested in determining if the preexisting methylation found in calf thymus H3 had any effect on the kinetics of H3 methylation compared to the unmodified H3.

Initial rate kinetics were carried out with CARM1 using both calf thymus and recombinant chick H3 (Figure 6). Plots of reaction rate vs histone concentration appear to be almost identical for the two histones. With each substrate, methylation rates reached a maximum of 4500 pmol min^{-1} (mg of enzyme)$^{-1}$, which is similar to what we observed for methylation of synthetic peptide R1 by PRMT1 (3100 pmol min^{-1} mg^{-1}). The histone concentration resulting in half-maximal rates of methylation, a gauge of binding affinity, was estimated to be ≤0.2 μM for both sources of H3. A Lineweaver−Burk plot of these data was not linear; as the concentration of H3 was dropped below 0.3 μM, initial rates were progressively lower than expected from an extrapolation of the data at higher H3 concentrations; thus the actual K_m may be lower than suggested by Figure 6. Despite the

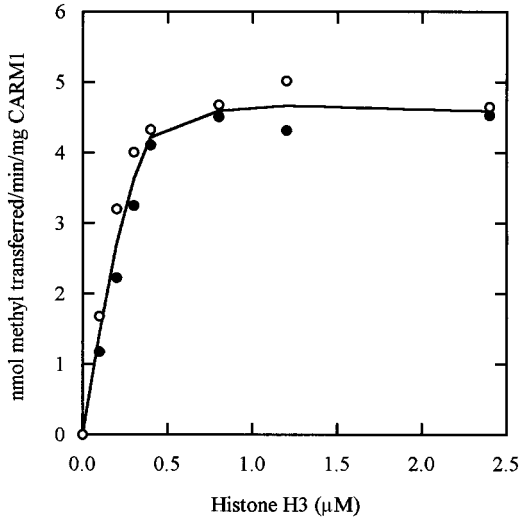

FIGURE 6: Effect of histone H3 concentration on initial rates of methylation by GST-CARM1. Reactions with calf thymus (○) and recombinant chicken (●) H3 were carried out according to method C in Table 1. Reactions were stopped by TCA precipitation and processed for liquid scintillation counting as described in Experimental Procedures.

complex nature of initial rate data, it is clear that CARM1 interacts effectively in vitro with recombinant histone H3 at concentrations of H3 well below 1 μM and that the preexisting methylation seen in calf thymus H3 has little, if any, effect on this interaction.

Identification of Major CARM1-Catalyzed Methylation Sites in Recombinant Chick H3. To identify the major sites of methylation catalyzed by CARM1, 1.5 nmol of recombinant chick H3 was methylated by method D in Table 1 to a stoichiometry of approximately 0.7 mol of CH_3/mol of histone in the presence of [^{3}H]Adomet, precipitated with trichloroacetic acid (TCA) to remove unreacted [^{3}H]Adomet, and then digested with endoproteinase Lys-C. Separation of the resulting peptides by reversed-phase HPLC and distribution of the associated radiolabel are shown in Figure 7, panel II. For comparison, panel I shows a separation of peptides derived from a Lys-C digest "standard" of the 1−50 fragment only of unmethylated recombinant chick H3. The identity of each peptide peak, as determined by MALDI-TOF mass spectrometry, is indicated. Peaks A, B, and C from panel II were independently pooled and then analyzed by high-resolution MALDI-TOF mass spectrometry (Figure 8 and Table 4). All three peaks were analyzed two to three times each over the entire range of masses expected for any arginine-containing peptide in a Lys-C digest of the complete H3 sequence. Peak A contained three peptides: an unmethylated version of the H3 fragment consisting of residues 15−18, a dimethylated version of H3 fragment 24−27, and a dimethylated version of H3 fragment 1−4 (see Figure 10 for the complete sequence of histone H3). The presence of these fragments in peak A is consistent with the peptide map standard seen in panel I. In the case of peptides 24−27 and 1−4, it is apparent that a considerable increase in retention time has occurred as a result of their dimethylation. Peak B contained only the dimethylated version of residues 15−18, again consistent with a methylation-dependent shift to later retention times. Peak C contained dimethylated, unmethylated, and monomethylated versions of residues 123−135, with relative abundance in the order indicated. Taken

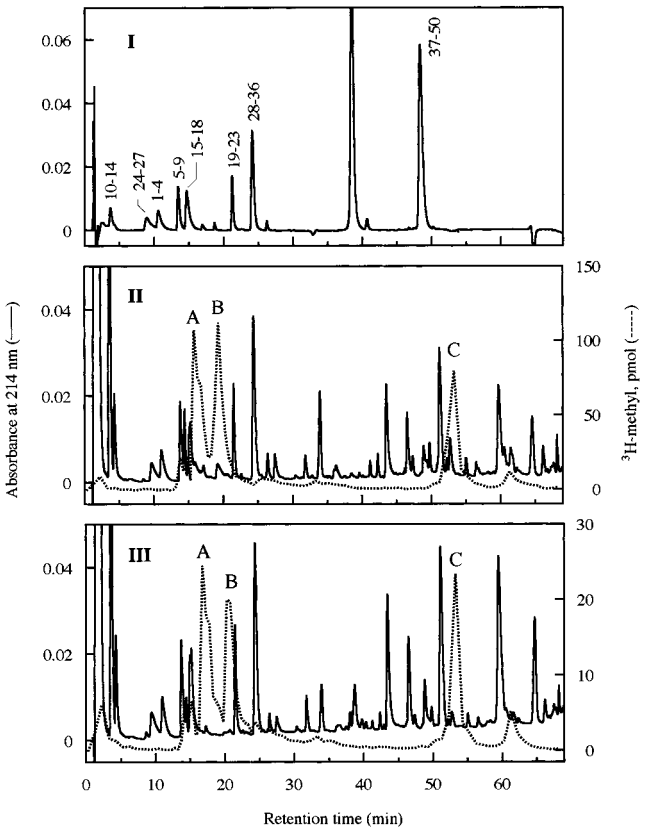

FIGURE 7: Reversed-phase HPLC of ^{3}H-methylated histone H3 after digestion with endoproteinase Lys-C. Panels II and III show peptide maps representing 1.3 nmol of H3 that was ^{3}H-methylated according to assays D and E, respectively, in Table 1. Despite a 5-fold difference in the overall extent of H3 methylation, the patterns of [^{3}H]methyl incorporation are nearly identical, with both digests yielding three major peaks (A, B, and C) of radiolabel incorporation. Panel I shows a peptide map obtained after Lys-C digestion of the H3(1−50) peptide obtained from unmethylated recombinant H3 after Glu-C digestion. Peak identities shown in panel I were obtained by mass spectrometry and used as a guide for determining possible candidate peptides responsible for major peaks of radiolabel seen in panels II and III. For all three panels, HPLC was carried out by method E in Table 2.

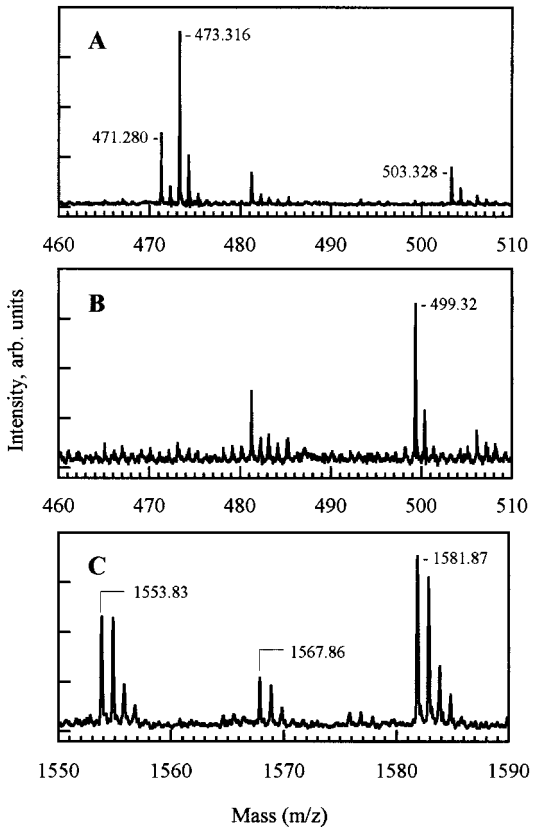

FIGURE 8: Identification of the major H3 methylation sites seen in Figure 7. Samples of peaks A, B, and C from panel II of Figure 7 were subjected to MALDI-TOF mass spectrometry in the high-resolution reflector mode as described in Experimental Procedures. Monoisotopic masses are labeled. The family of peaks observed in the mass range of 481−485 seen in panels A and B was also observed in a matrix-only blank run.

Table 4: Mass Analysis of Peaks A, B, and C from Figure 7[a]

				mass $[M + H]^+$		
peak	peptide	sequence	Me	obsd	expected	Δ
A	15−18	APRK	0	471.280	471.304	−0.024
A	24−27	AARK	2	473.316	473.320	−0.004
A	1−4	ARTK	2	503.328	503.331	−0.003
B	15−18	APRK	2	499.320	499.336	−0.016
C	123−135	DIQLARRIRGERA	0	1553.83	1553.898	−0.07
C	123−135	DIQLARRIRGERA	1	1567.86	1567.914	−0.05
C	123−135	DIQLARRIRGERA	2	1581.87	1581.930	−0.06

[a] MALDI-TOF mass analysis was carried out in the positive ion, reflector mode using internal standards. Masses are monoisotopic. Column 4 (Me) indicates the methylation state.

together, these results demonstrate that significant dimethylation occurs on arginine residues 2, 17, and 26 within the N-terminal region of histone H3. Within the first 37 residues of H3, the only arginine not found by mass analysis to be methylated was Arg-8. This result was surprising given that Arg-8 and Arg-26 occur within the same four-residue sequence, -ARKS-. On the basis of the standard peptide map in panel I and the retention shift behavior of peptides 1−4, 15−18, and 24−27, one would expect that mono- or dimethylated forms of 5−8 (if they were present) would elute with peaks A and/or B of panel II. Despite repeated attempts to detect mono- or dimethylated peptide 5−9, no evidence was found by mass analysis for either one in peaks A or B.

As an independent check on the methylation status of Arg-8, we carried out radiosequencing of ^{3}H-methylated chick H3 (Figure 9). These results confirmed what we had found by mass spectrometry; significant methylation occurs at Arg-2 and Arg-17, but relatively little methylation occurs at Arg-8.

The methylation reaction used to generate the peptide map seen in panel II of Figure 7 was designed to maximize the extent of histone modification by CARM1. Although these conditions facilitate the analysis of methylation sites by producing high yields of methylated peptides, they run the risk of obscuring relative site preferences that might occur in vivo. To address this concern, we also methylated H3 to a lower stoichiometry using less CARM1 and a shorter incubation time. As shown in panel III of Figure 7, these conditions succeeded in lowering methylation of H3 to about one-fifth of that seen in panel II. Despite this lower level of modification, the overall pattern of methyl incorporation into peaks A, B, and C was remarkably unchanged. Of particular interest is the fact that peak C remains a major contributor in panel III, suggesting that methylation at the C-terminus of H3 occurs with an efficiency comparable to that of sites in the N-terminal region.

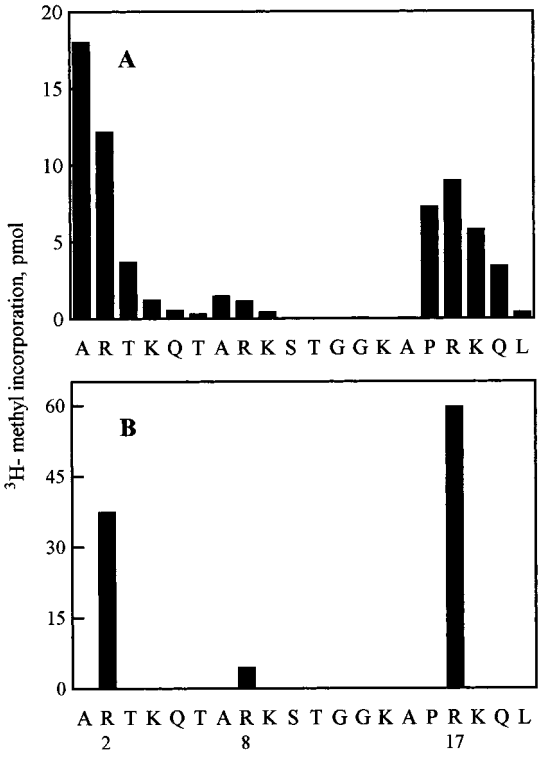

FIGURE 9: Radiosequencing of residues 1−20 of ^{3}H-methylated H3. Recombinant H3 (1.5 nmol) was ^{3}H-methylated per method D in Table 1 and purified by HPLC method B in Table 2. Radiosequencing was carried out on 405 pmol of methylated H3 as described in Experimental Procedures. The raw data are shown in panel A. Amino acid sequencing carried out for three cycles on a small portion of this same material revealed that 40−60% of the H3 was missing the expected alanine residue at the N-terminus, presumably due to the action of a contaminating protease during the prolonged methylation reaction. Panel B shows a refinement of the data from panel A in which correction is made for the ragged N-terminus, for sequencing lag, and for an assumed repetitive yield of 95%. To make this refinement, we first corrected all of the data in panel A for repetitive yield and then combined the radiolabel yields as follows: Arg-2 (sum of 1−6), Arg-8 (sum of 7−9), and Arg-17 (sum of 16−20).

```
 Δ                Δ         Δ
ARTKQTARKSTGGKAPRKQLATKAARKSAPATGGVKKPHR
         10        20        30        40

YRPGTVALREIRRYQKSTELLIRKLPFQRLVREIAQDFKT
         50        60        70        80

DLRFQSSAVMALQEASEAYLVGLFEDTNLCAIHAKRVTIM
         90       100       110       120

      {ΔΔ Δ  Δ}
PKDIQLARRIRGERA
        130
```

FIGURE 10: Sequence of histone H3 (chicken) showing major CARM1 methylation sites. Methylation sites determined in this study are indicated by the symbol (△) above the relevant arginine residue. Two of these sites, Arg-17 and Arg-26, occur in a possible consensus sequence, -KAXRK-, which is underlined. Methylation at the C-terminus occurs on one or more of the four marked residues.

DISCUSSION

H3 Has the Properties Expected of a Physiological Substrate for CARM1. Using two different methyl-accepting substrates, synthetic peptide R1 and histone H3, we found that CARM1 methylates arginine but not lysine residues. In the case of H3, methylation produced ADMA and MMA with little or no SDMA. This latter finding, together with its previously reported cDNA sequence, indicates that CARM1 belongs to the same family of protein arginine methyltransferases as PRMT1, which currently serves as the archetype for this class of methyltransferase (*5*).

The high catalytic activity of CARM1 toward H3 is similar to that exhibited by PRMT1 toward peptide R1. Moreover, the apparent K_m of CARM1 toward histone H3 is in the submicromolar range. These favorable kinetic properties suggest that H3 may be a physiological target of CARM1 action in vivo or that it closely resembles such targets.

Additional evidence that H3 may be methylated in vivo on arginine residues is afforded by our finding that acid hydrolysates of calf thymus H3 contain significant, albeit low, levels of ADMA and/or MMA. It is interesting to note that the methylarginine content of H3 (3.7%) was higher, by a factor of 4, than any of the other core histones. The low level of preexisting arginine methylation explains why almost no difference is seen in the methylation kinetics of calf thymus vs recombinant chick H3. The low level of preexisting arginine methylation seen in calf thymus H3 is consistent with a role for arginine methyltransferases in selective gene transcription. As with lysine acetylation, arginine methylation might be a reversible modification, contributing further to a low steady-state level of this modification in cells.

Site Specificity of CARM1. Most of the posttranslational modifications known to occur in core histones are found in the first 28 residues of the flexible N-termini (*7*, *8*). H3, one of the two arginine-rich core histones, contains a total of 18 arginines, of which 4 fall within the first 28 residues at positions 2, 8, 17, and 26 (Figure 10). We estimate that CARM1 catalyzed the following distribution of methyl group additions within the N-terminus: Arg-2 (6%); Arg-17 (35%); Arg-26 (29%). We arrived at these numbers by estimating the relative areas of peaks A, B, and C in Figure 7, panel II, to be 35%, 35%, and 30%, respectively. Within peak A, we assigned values of 6% and 29% to sites 2 and 26, respectively, on the basis of the relative heights of the mass detector responses for peptides 1−4 and 24−27 in panel A of Figure 8. The relative percentages calculated for Arg-2 and Arg-17 may appear inconsistent with the sequencing analysis presented in Figure 9, in which panel B shows Arg-17 with 60% more methyl incorporation than Arg-2. Note, however, that, in creating panel B of Figure 9, we assumed a favorable repetitive yield of 95%, which is typical for many sequencers working under optimal conditions. Because overall yields drop exponentially from cycle to cycle, a relatively small error in the repetitive yield assumption can make a large difference in calculated stoichiometries of site modification, especially when two sites that are widely separated within in given sequencing run are compared. If our repetitive yields are assumed to be in the range of 85−90%, a likely possibility in our opinion, then the ratio of Arg-17 to Arg-2 methylation approaches the value of 6:1, consistent with the relative contributions of these two sites calculated above. Neither mass detector peak heights nor sequencing yields are ideal for quantifying relative site occupancies. In this instance, however, we feel the mass detector data provide a useable and significantly more accurate estimate, especially since the size and composition of the two peptides being

compared (1−4 and 24−27) are very similar and the data were obtained simultaneously from the same sample.

It is clear from Figure 9, as well as from our inability to detect a methylated 5−9 fragment, that Arg-8 is a minor site of methylation at best. This is somewhat surprising given that Arg-8 and Arg-26 occur in an identical four-residue sequence, -ARKS-. On the other hand, it is not surprising that Arg-17 and Arg-26 exhibit similar methylation levels as both occur in highly similar five-residue sequences having the common pattern -KAXRK-.

The remaining 30% of methyl incorporation occurs at one or more of the four clustered arginine residues (128/129/131/134) near the C-terminus. None of these four residues occurs in a -KAXRK- sequence, but one of them, Arg-131, falls in a sequence that has a basic residue in the −3 position, as do Arg-17 and Arg-26 but not Arg-2 or Arg-8.

It is of great interest to know if selective methylation of H3 by CARM1 occurs in vivo, and if so, if the site selectivity is the same as reported here with isolated H3. As an approach to this question, we have attempted to methylate purified rat nucleosomes with CARM1 but found no significant methylation of H3. It may be that the relevant methylation sites of H3 are inaccessible to CARM1 in the nucleosome unless the appropriate combination of transcription factors and related proteins is present. Precedent for this has been documented in the case of yeast GCN5, a transcriptional coactivator in yeast that acetylates histone H3 in vivo. Acetylation of H3 in purified yeast nucleosomes is observed only when the appropriate complex of accessory factors is present (*20*). Direct assessment of in vivo arginine methylation of H3 in mammalian cells may be addressed by the use of antibodies that selectively discriminate between methylated and unmethylated forms of H3. Attempts to raise such antibodies, utilizing the site specificity demonstrated here with purified H3, are currently in progress.

Histone Methylation and Gene Regulation. Until recently, histone methylation has generally taken a back seat to acetylation and phosphorylation as a contributor to dynamic regulation of nucleosome structure and gene expression. The static role for methylation fits well with observations that methyl turnover is generally hard to distinguish from histone turnover and that, unlike the cases of acetylation and phosphorylation, there are no well-documented enzymes that reverse histone methylation, either at lysine or at arginine residues. Intriguing exceptions to the static model include a 1988 paper by Desrosiers and Tanguay (*10*), who reported that heat shock of *Drosophila* cells in culture led to a rapid increase in methylated arginine in H3, in concert with a reduction in methylated lysine, and a 1994 paper by Annunziato and co-workers (*21*), who used metabolic labeling of histones in HeLa cells to demonstrate a subclass of methylation sites in histone H3 that appears to turn over much more rapidly than methylation sites on other histones. The discovery of CARM1 last year provided the first clear link between transcriptional regulation and methyltransferase activity (*1*). More recently, Strahl and Allis (*22*) demonstrated that methylation of lysine 4 in histone H3 is associated almost exclusively with active chromatin in *Tetrahymena*, while Rea et al. (*23*) have found evidence that methylation of lysine 9 in human H3 influences, and is itself influenced by, other covalent modifications in the N-terminal region.

FIGURE 11: Sequence of the histone H3 (chicken) N-terminal region showing the relationship of known acetylation, phosphorylation, and methylation sites. The following symbols are used: (Δ) arginine methylation from this study; (◊) lysine methylation; (Ω) lysine acetylation; (*) serine phosphorylation. Locations of the latter three modifications are based on the recent review of Strahl and Allis (*7*). Our proposed CARM1 recognition sequences are typed in bold.

Recent reviews have emphasized the emerging role for multiple/interdependent posttranslational modifications at histone N-termini in regulating gene expression via perturbation of histone−DNA interactions and/or formation of unique binding domains on histones that could attract additional coactivators which fine-tune the efficiency and selectivity of transcription (*7*, *8*). The studies on H3 methylation by CARM1 presented here raise further the level of potential information content coded by N-terminal modifications (Figure 11). In this regard it is interesting to calculate the maximum number of modification states that could occur within the 1−28 region of H3 on the basis of acetylation or methylation of lysine, methylation of arginine, and phosphorylation of serine. In doing so, we consider that any lysine in this region can exist in five different states (unmodified, acetylated, or three levels of methylation), that the arginines can exist in three states (unmodified, two levels of methylation), and that the serines can be unmodified or phosphorylated. These assumptions provide a total of over 4×10^6 states. Even if we allow for a high degree of degeneracy among the superset of modification states, there is still enormous capacity for molecular decision making in just the N-terminus of H3.

While most discussions of histone modification focus on the N-termini, we found that a significant percentage of the CARM1-catalyzed methylation of H3 occurred at the C-terminus, even when methylation was held to a low level (panel III vs panel II of Figure 7). The three-dimensional nucleosome structures derived from X-ray diffraction data (*14*, *24*, *25*), and antibody mapping of histone accessible residues (*26*), suggest that the extreme C-terminus may also be accessible for modification. The C-termini of the two H3 molecules within a nucleosome butt up against each other and constitute a "hinge" region around which the superhelical horseshoe-shaped H3/H4 tetramer can twist from a left-handed to a right-handed configuration. It has been suggested that this helical flipping may play a physiological role in altering the accessibility of the nucleosomal DNA for transcription (*27*). Methylation of one or more H3 C-terminal arginines by CARM1 might facilitate this flipping by destabilizing side-chain interactions within the critical hinge region.

It has been reported that Arg-128, Arg-129, and Arg-131 of H3 can be phosphorylated by a Ca^{2+}/calmodulin-dependent protein kinase from mouse leukemia cells (*28*). If methylation and/or phosphorylation of the C-terminal arginines prove(s) to be physiologically important, this will greatly increase the coding potential of histone H3.

REFERENCES

1. Chen, D., Ma, H., Hong, H., Koh, S. S., Huang, S.-M., Schurter, B. T., Aswad, D. W., and Stallcup, M. R. (1999) *Science 284*, 2174−2177.
2. Xu, L., Glass, C. K., and Rosenfeld, M. G. (1999) *Curr. Opin. Genet. Dev. 9*, 140−147.
3. Tang, J., Frankel, A., Cook, R. J., Kim, S., Paik, W. K., Williams, K. R., Clarke, S., and Herschman, H. R. (2000) *J. Biol. Chem. 275*, 7723−7730.
4. McBride, A. E., Weiss, V. H., Kim, H. K., Hogle, J. M., and Silver, P. A. (2000) *J. Biol. Chem. 275*, 3128−3136.
5. Gary, J. D., and Clarke, S. (1998) *Prog. Nucleic Acid Res. Mol. Biol. 61*, 65−131.
6. Scott, H. S., Antonarakis, S. E., Lalioti, M. D., Rossier, C., Silver, P. A., and Henry, M. F. (1998) *Genomics 48*, 330−340.
7. Strahl, B. D., and Allis, C. D. (2000) *Nature 403*, 41−45.
8. Spencer, V. A., and Davie, J. R. (1999) *Gene 240*, 1−12.
9. Wade, P. A., Pruss, D., and Wolffe, A. P. (1997) *Trends Biochem. Sci. 22*, 128−132.
10. Desrosiers, R., and Tanguay, M. (1988) *J. Biol. Chem. 263*, 4686−4692.
11. Duerre, J. A., and Buttz, H. R. (1990) in *Protein Methylation* (Paik, W. K., and Kim, S., Eds.) pp 125−138, CRC Press, Boca Raton, FL.
12. Najbauer, J., Johnson, B. A., Young, A. L., and Aswad, D. W. (1993) *J. Biol. Chem. 268*, 10501−10509.
13. Chirpich, T. P. (1968) Lysine 2,3-aminomutase; Purification and Properties, Ph.D. Dissertation, University of California, Berkeley.
14. Harp, J. M., Uberbacher, E. C., Roberson, A. E., Palmer, E. L., Gewiess, A., and Bunick, G. J. (1996) *Acta Crystallogr., Sect. D: Biol. Crystal. 52*, 283−288.
15. Jones, B. N., Pääbo, S., and Stein, S. (1981) *J. Liq. Chromatogr. 4*, 565−586.
16. Lowry, O. H., Rosebrough, N. J., Farr, A. L., and Randall, R. J. (1951) *J. Biol. Chem. 193*, 265−275.
17. Lin, W. J., Gary, J. D., Yang, M. C., Clarke, S., and Herschman, H. R. (1996) *J. Biol. Chem. 271*, 15034−15044.
18. Gary, J. D., Lin, W. J., Yang, M. C., Herschman, H. R., and Clarke, S. (1996) *J. Biol. Chem. 271*, 12585−12594.
19. DeLange, R. J., Hooper, J. A., and Smith, E. L. (1973) *J. Biol. Chem. 248*, 3261−3274.
20. Grant, P. A., Schieltz, D., Pray-Grant, M. G., Steger, D. J., Reese, J. C., Yates, J. R., and Workman, J. L. (1998) *Cell 94*, 45−53.
21. Annunziato, A. T., Eason, M. B., and Perry, C. A. (1995) *Biochemistry 34*, 2916−2924.
22. Strahl, B. D., Ohba, R., Cook, R. G., and Allis, C. D. (1999) *Proc. Natl. Acad. Sci. U.S.A. 96*, 14967−14972.
23. Rea, S., Eisenhaber, F., O'Carroll, D., Strahl, B. D., Sun, Z.-W., Schmid, M., Opravil, S., Mechtler, K., Ponting, C. P., Allis, C. D., and Jenuwein, T. (2000) *Nature 406*, 593−599.
24. Arents, G., Burlingame, R. W., Wang, B.-C., and Love, W. E. (1991) *Proc. Natl. Acad. Sci. U.S.A. 88*, 10148−10152.
25. Luger, K., Mäder, A. W., Richmond, R. K., Sargent, D. F., and Richmond, T. J. (1997) *Nature 389*, 251−260.
26. Stemmer, C., Briand, J. P., and Muller, S. (1997) *J. Mol. Biol. 273*, 52−60.
27. Hamiche, A., Carot, V., Alilat, M., De Lucia, F., O'Donohue, M. F., Revet, B., and Prunell, A. (1996) *Proc. Natl. Acad. Sci. U.S.A. 93*, 7588−7593.
28. Wakim, B. T., and Aswad, G. D. (1994) *J. Biol. Chem. 269*, 2722−2727.

BI002631B